

Magnetic properties of the Haldane-gap material NENB

E. Čízmár,* M. Ozerov, O. Ignatchik, T. P. Papageorgiou, J. Wosnitza, and S. A. Zvyagin
*Dresden High Magnetic Field Laboratory (HLD),
Forschungszentrum Dresden-Rossendorf, 01314 Dresden, Germany*

J. Krzystek

National High Magnetic Field Laboratory, Florida State University, Tallahassee, FL 32310, USA

Z. Zhou

Department of Physics and Astronomy, Wayne State University, Detroit, MI 48201, USA

C. P. Landee, B. R. Landry, and M. M. Turnbull

Department of Physics and Carlson School of Chemistry, Clark University, Worcester, MA 01060, USA

J. L. Wikaira

Department of Chemistry, University of Canterbury, Christchurch, New Zealand

(Dated: February 5, 2008)

Results of magnetization and high-field ESR studies of the new spin-1 Haldane-chain material $[\text{Ni}(\text{C}_2\text{H}_8\text{N}_2)_2\text{NO}_2](\text{BF}_4)$ (NENB) are reported. A definite signature of the Haldane state in NENB was obtained. From the analysis of the frequency-field dependence of magnetic excitations in NENB, the spin-Hamiltonian parameters were calculated, yielding $\Delta = 17.4 \text{ K}$, $g_{||} = 2.14$, $D = 7.5 \text{ K}$, and $|E| = 0.7 \text{ K}$ for the Haldane gap, g factor and the crystal-field anisotropy constants, respectively. The presence of fractional $S = 1/2$ chain-end states, revealed by ESR and magnetization measurements, is found to be responsible for spin-glass freezing effects. In addition, extra states in the excitation spectrum of NENB have been observed in the vicinity of the Haldane gap, which origin is discussed.

PACS numbers: 76.30.-v, 74.25.Ha, 75.50.Gg, 75.30.Gw

Antiferromagnetic (AFM) quantum spin-1 chains have been the subject of intense theoretical and experimental studies, fostered especially by the Haldane conjecture.¹ In accordance to the valence-bond-solid (VBS) model proposed by Affleck *et al.*², each $S = 1$ spin can be regarded as a symmetric combination of two $S = 1/2$ moments forming a spin-singlet ground state. The value of the energy gap $\Delta = 0.41J$ (where J is the spin-spin exchange coupling) has been estimated for an $S = 1$ isotropic Heisenberg AFM chain using the density-matrix renormalization-group (DMRG)³ and exact diagonalization⁴ techniques. The presence of the Haldane gap was experimentally revealed in a number of materials (see for instance Ref. 5,6,7,8). Nowadays, investigations of intriguing properties of Haldane materials (particular their high-field magnetic properties) continue to attract a great deal of attention. For instance, experimental studies of the Haldane materials NDMAP^{9,10} and TMNIN¹¹ suggest the realization of the Tomonaga-Luttinger-liquid high-field phase.^{12,13} At sufficiently low temperature, an applied magnetic field can induce long-range magnetic order, which can be effectively described as the condensation of a dilute gas of magnons.^{14,15}

In this paper, we utilize magnetization and electron spin resonance (ESR) techniques to study the new spin-1 Haldane compound $[\text{Ni}(\text{C}_2\text{H}_8\text{N}_2)_2\text{NO}_2](\text{BF}_4)$ (abbreviated as NENB). The presence of the Haldane state in NENB has been confirmed experimentally. Analy-

sis of the frequency-field dependence of magnetic excitations in NENB allowed us to determine the spin-Hamiltonian parameters, yielding $g_{||} = 2.14$, $D = 7.5 \text{ K}$, and $|E| = 0.7 \text{ K}$ for the g factor and the crystal-field anisotropy constants, respectively. The presence of spin-1/2 excitations in nominally pure NENB crystals revealed by our experimental observations suggested the existence of weakly-interacting antiferromagnet droplets originating from broken spin bonds. In addition, extra states in the excitation spectrum in the vicinity of the Haldane gap were observed, which origin is discussed.

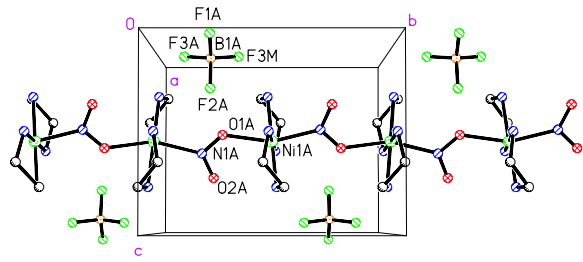


FIG. 1: (Color online) The structure of NENB showing the polymeric chain arrangement, the orientation of the nitrite ligands, and the placement of the BF_4 anions relative to the chain. Atoms are shown as spheres of arbitrary size and hydrogen atoms are not shown for clarity.

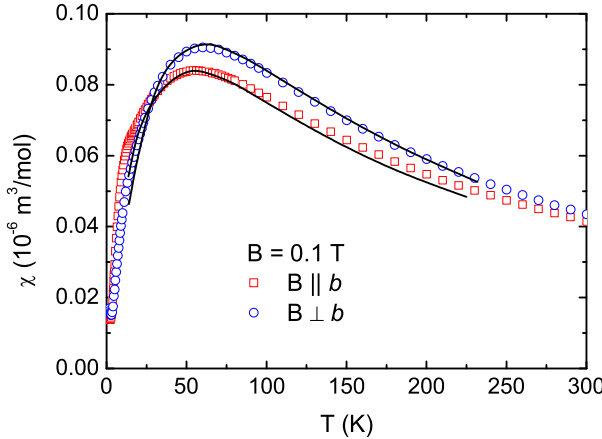


FIG. 2: (Color online) Magnetic susceptibility of NENB measured in a magnetic field of 0.1 T, applied along (squares) and perpendicular (circles) to the b axis. The solid lines represent calculations using the $S = 1$ Heisenberg AFM chain model with $D/J = 0.2$ (see the text for details).

Single crystals of NENB were grown by the reaction of $[\text{Ni}(\text{C}_2\text{H}_8\text{N}_2)_3](\text{BF}_4)_2$ with $\text{Ni}(\text{BF}_4)_2 \cdot 6\text{H}_2\text{O}$ and NaNO_2 in aqueous solution. Careful, slow evaporation in a partially covered container yielded ruby-red crystals of up to 3-4 mm in length and 1-2 mm² cross section. Single-crystal X-ray analysis showed an orthorhombic unit cell, space group $Pnma$ (similar to that of the isostructural compound NENP¹⁶), with $a = 15.0373(5)$ Å, $b = 10.2276(3)$ Å, and $c = 7.9719(2)$ Å. Each Ni^{2+} ion is pseudo-octahedrally coordinated. The four nitrogen atoms of the two ethylenediamine rings (ethylenediamine = $\text{C}_2\text{N}_2\text{H}_8$) make a slightly distorted square planar symmetry with bridging NO_2^- ions creating the octahedral axis approximately parallel to the chain direction. The individual chains are well isolated by the inorganic counterions BF_4^- . As follows from crystallographic analysis the mean planes of successive Ni^{2+} units are canted by an angle of 14.1° to each other. The orientation of the nitrite ions within a single chain appears to be uniform (one N atom and one O atom are coordinated to each Ni^{2+} center) as shown in Fig. 1 (full crystallographic details are available from the Cambridge Crystallographic Data Center, deposition number 637023).¹⁷

The static susceptibility was measured using a commercial SQUID magnetometer equipped with a 7-Tesla magnet in the temperature range from 1.8 to 300 K. The sample was attached with a small amount of Apiezon N grease to the inside of a straw held by a sample-holder rod. The core diamagnetic contribution to the magnetic moment of the sample, calculated using Pascal's constants,¹⁸ was subtracted from the raw data. The magnetization was measured in fields up to 15 T using a torque magnetometer in a dilution refrigerator. ESR experiments were performed in the Voigt geometry with the external field applied along the b axis using a tunable-frequency ESR setup at the National High Mag-

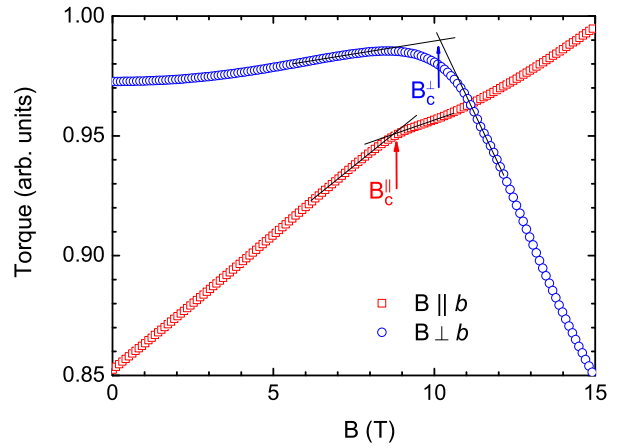


FIG. 3: (Color online) Field dependence of the magnetic torque of NENB at 20 mK for two field orientations.

netic Field Laboratory, Tallahassee.¹⁹

The zero-field-cooled magnetic susceptibility of NENB measured in a field of $B = 0.1$ T applied parallel and perpendicular to the b axis is shown in Fig. 2. The pronounced maximum and low-temperature behavior of the magnetic susceptibility suggest a spin-singlet ground state, which is a characteristic property of $S = 1$ Haldane systems. Due to anisotropy effects, the position of the susceptibility maximum depends on the field orientation. The existence of a finite crystal-field anisotropy in NENB has been confirmed by low-temperature (20 mK) magnetization measurements using the torque magnetometry technique. Two critical fields ($B_c^{\parallel} \sim 9$ T and $B_c^{\perp} \sim 10$ T for B applied parallel and perpendicular to the b axis, respectively) were resolved in the magnetization data (Fig. 3), suggesting a field-induced collapse of the spin-singlet ground state for both orientations of the magnetic field. The critical fields revealed in our experiments agree well with those obtained from optical and magnetization measurements.¹⁷

To get a deeper insight into the peculiarity of magnetic interactions in NENB, tunable-frequency ESR measurements have been performed in magnetic fields up to 16 T. The excitation spectrum of NENB in fields parallel to the b axis (which is the chain axis) is plotted in Fig. 4. Several ESR modes have been observed. In order to assign these modes to field-dependent transitions in the energy scheme of magnetic excitations we analyzed the data using the effective Hamiltonian, written as²⁰

$$\mathcal{H} = \Delta + D'(S_i^z)^2 + E'[(S_i^x)^2 - (S_i^y)^2] - \mu_B S g B \quad (1)$$

with eigenstates of type $|S, S^z\rangle$, where Δ is the Haldane gap, D' and E' represent reduced parameters of the crystal field anisotropy (uniaxial- and rhombic-distortion parameters, respectively) of the Ni ions, while the last term is the Zeeman energy for an ion with $S = 1$.

The field-dependent energy scheme (Fig. 5) corresponding to this Hamiltonian allows one to understand

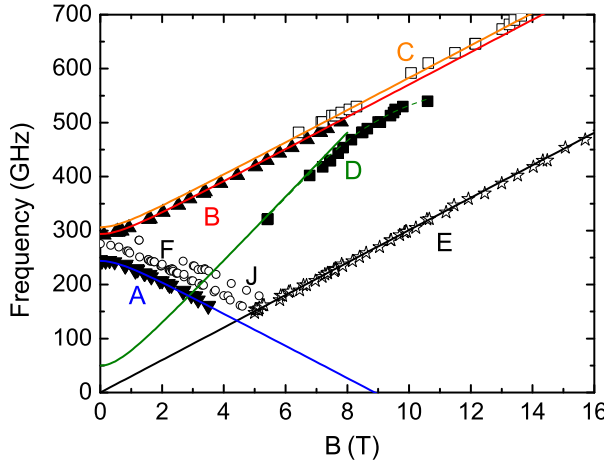


FIG. 4: (Color online) Field dependence of the magnetic ESR excitations of NENB observed at 1.5 K with the magnetic field aligned along the b axis. Solid lines represent the fit of effective Hamiltonian (Eq. 1) to the experimental data.

most of the observed ESR modes. First, the transitions from the ground state to the first excited states ($|0, 0\rangle \rightarrow |1, \pm 1\rangle$), denoted by A and B, have been observed in fields up to ~ 8 T as shown by the triangles in Fig. 4. The extrapolation of the mode A to zero frequency suggests the existence of a critical field $B_c^{\parallel} \approx 9$ T, which coincides nicely with the change of the torque signal for fields applied parallel to the b axis (Fig. 3). At this field, the first excited level crosses the nonmagnetic ground state transforming the system into a state with a finite magnetization. The transitions A and B would be forbidden in a system with purely axial symmetry, but can be allowed in the presence of a staggered magnetization.²¹ As suggested by Sakai and Shiba²², the staggered term lifts wave-vector selection rules and allows transitions from the ground states to the excited states at the boundaries of the Brillouine zone. The staggered magnetic moment may originate from an alternating g tensor (which was revealed by crystallographic analysis of NENB) or a finite Dzyaloshinskii-Moriya interaction.

The mode D corresponds to transitions $|1, -1\rangle \rightarrow |1, 1\rangle$, which are only allowed in the presence of the broken axial symmetry. As follows from our ESR data, the excited doublet is split in zero magnetic field, which is a clear signature of a finite rhombic distortion. The mode C corresponds to $|1, -1\rangle \rightarrow |1, 0\rangle$ transitions observed in fields above ~ 6 T. The observation of this excitation mode is of particular importance, since it gives direct evidence for the four-level excitation scheme, which is a typical feature of an $S = 1$ Haldane-chain system with finite anisotropy. Then, in accordance to Eq. 1 for the Haldane gap we found $\Delta = 17.4$ K.

Two more resonance absorptions (the modes F and J, Fig. 4) have been observed in the low-temperature excitation spectrum of NENB. The field dependences of these excitations are similar to that of mode A. The excitation

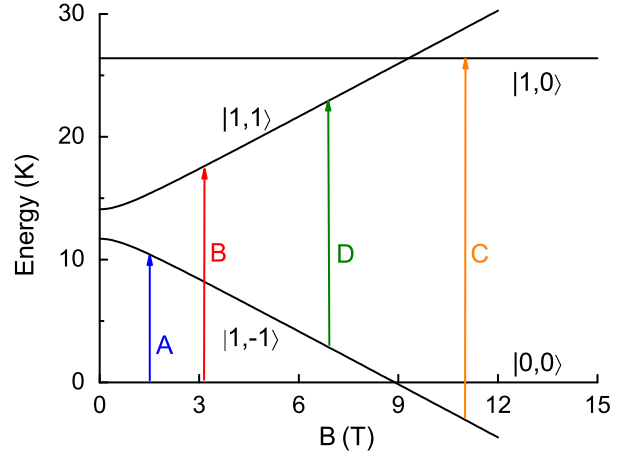


FIG. 5: (Color online) Proposed field-dependent energy scheme of NENB (using Eq. 1) for magnetic fields applied along the b axis.

energies are higher by 30 and 60 GHz, for the modes F and J, respectively. The origin of these excitations is not clear at the moment. As mentioned above, the orientation of the nitrite ions within a single chain appears to be uniform (one N atom and one O atom are coordinated to Ni^{2+} center along the chain direction). On the other hand, as mentioned in Ref. 23, one can not exclude the possibility of two additional, minor Ni^{2+} sites within the chains caused by the reversal of the orientation of the NO_2^- groups. This would lead to occasional positions where a Ni^{2+} ion in NENB would have either two O atoms from nitrite ions, or two N atoms from nitrite ions. Such a possibility was also suggested for the isostructural perchlorate compound NENP.¹⁶ It is important to mention here that additional states close to the Haldane gap were observed in NENP by means of high-field ESR,^{6,24} which is fully consistent with our observations. Another possible explanation of the extra states observed by us is the presence of effective ferromagnetic impurity-induced bonds as revealed by susceptibility measurements, see discussion below. Such bonds were found to be responsible for the splitting of the neutron scattering peak into two incommensurate parts placed symmetrically around the boundary of the Brillouine zone close to the gap energy in $\text{Y}_{2-x}\text{Ca}_x\text{BaNiO}_5$.²⁵ However, it is fair to mention that to prove this mechanism to be present in NENB requires more detailed investigations.

Finally, a strong resonance line E, with $g = 2.14$ was observed. The observation of the mode suggests the presence of spin-1/2 states (which origin can be ascribed to fractional chain-end effects or multiply frustrated inter-chain interactions) even in nominally pure samples of NENB. These effects, as suggested below, appear to affect the low-temperature magnetic susceptibility behavior.

Using the Hamiltonian Eq. 1, the ESR data can be fit with parameters $\Delta = 17.4$ K, $D' = -13.5$ K, $|E'| =$

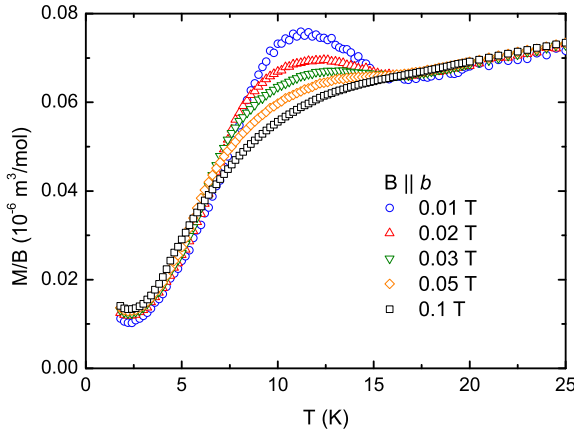


FIG. 6: (Color online) Temperature dependence of the magnetic susceptibility of NENB in different magnetic fields applying along the chain b axis.

1.2 K, and $g_{\parallel} = 2.14$. Numerical calculations for the diagonalization of the Hamiltonian of $S = 1$ anisotropic exchange-coupled spin-chain system

$$\mathcal{H} = -J \sum_i S_i S_{i+1} + \sum_i \{D(S_i^z)^2 + E[(S_i^x)^2 - (S_i^y)^2]\} - \sum_i \mu_B S_i g B, \quad (2)$$

outlined in Ref. 6 suggest the relations $D = -D'/1.8$ and $|E| = |E'|/1.7$, which yield crystal-field anisotropy parameters $D = 7.5$ K and $|E| = 0.7$ K.

Using the obtained set of parameters, the magnetic susceptibility has been fit by the high-temperature series expansion for the $S = 1$ AFM spin-chain model^{16,26} yielding $J = -44.8$ K, $g_{\parallel} = 2.15$ and $J = -47.7$ K, $g_{\perp} = 2.28$ for $B \parallel b$ and $B \perp b$, respectively. The relatively strong crystal-field anisotropy, $D = 7.5$ K, as estimated from our ESR data, yields a ratio $D/|J| = 0.17$. This suggests that another model (where the influence of anisotropy is taken into account) might be more appropriate for describing the magnetic susceptibility.²⁷ Although theoretical predictions are available for $D/|J| = 0.2$, the overall agreement with the experimentally determined susceptibility data is very good (see Fig. 2). We obtain $J = -45$ K, $g_{\parallel} = 2.15$ and $J = -46.5$ K, $g_{\perp} = 2.28$ for $B \parallel b$ and $B \perp b$, respectively. Combining these values of the exchange coupling with the ESR results for Δ we obtain $\Delta/|J|$ in the range from 0.39 to 0.42, which is in good agreement with theoretical predictions.^{3,4}

The presence of fractional $S = 1/2$ chain-end spins might be a possible explanation for the observation of

the resonance line E in the ESR spectrum as well as for a weak Curie-like low-temperature upturn observed in the susceptibility. The low-temperature susceptibility measured in magnetic fields from 0.01 to 0.1 T (applied parallel to the b axis) is shown in Fig. 6. The susceptibility is characterized by a small but clearly resolvable local maximum at ~ 12 K, which gets rapidly suppressed with increasing magnetic field. Such behavior can be accounted for by the formation of a spin-glass state that has been also observed in powdered NENB samples.²⁸

When structural defects or non-magnetic impurities are introduced in the spin chain, the VBS model predicts the presence of two unpaired $S = 1/2$ spins, one at each end of the open chain. The existence of these end-chain states has been confirmed numerically (using the Monte Carlo²⁹ and DMRG³⁰ calculations) as well as experimentally in the Haldane material NENP doped with non-magnetic ions.³¹ A pronounced signature of the $S = 1/2$ chain-end interaction is a spin-glass behavior, as observed by Hagiwara *et al.*^{32,33} who proposed a model where structural defects induce ferromagnetic bonds between the moments at the ends of finite chains. On the other hand, the structural defects would allow a stronger interchain coupling at the defect sites, which assuming a random distribution of defects appears to induce frustrations and the spin-glass behavior. Additional impurity-induced energy levels were calculated and observed in the quasi-one-dimensional Heisenberg-chain compound $Y_{2-x}Ca_xBaNiO_5$.^{25,34}

In conclusion, a systematic study of the new spin-1 AFM Heisenberg-chain system NENB has been presented. We showed conclusively, that NENB belongs to the Haldane class of materials, with the energy gap $\Delta = 17.4$ K. Based on the analysis of the ESR and magnetization data, the spin-Hamiltonian parameters have been estimated, yielding the exchange coupling $J = -45$ K and crystal-field anisotropy parameters $D = 7.5$ K and $|E| = 0.7$ K. Extra states in the vicinity of the Haldane gap were observed, which origin is discussed. The presence of fractional $S = 1/2$ chain-end moments, revealed by means of ESR and magnetization measurements, is found to be responsible for spin-glass freezing effects, which is consistent with the VBS model for $S = 1$ Heisenberg AFM chains.

The authors would like to thank I. Affleck for fruitful discussions. Part of this work was supported by the DFG (project No. ZV 6/1-1). Part of this work was performed at the National High Magnetic Field Laboratory, Tallahassee, USA, which is supported by NSF Cooperative Agreement No. DMR-0084173, by the State of Florida, and by the DOE. S.A.Z. acknowledges the support from the NHMFL through the VSP No. 1382.

* Electronic address: e.cizmar@fzd.de

¹ F. D. M. Haldane, Phys. Rev. Lett. **50**, 1153 (1983).

- ² I. Affleck, T. Kennedy, E. H. Lieb, and H. Tasaki, Phys. Rev. Lett. **59**, 799 (1987).
- ³ S. R. White and D. A. Huse, Phys. Rev. B **48**, 3844 (1993).
- ⁴ O. Gollineli, T. Jolicoeur, and R. Lacaze, Phys. Rev. B **50**, 3037 (1994).
- ⁵ J. P. Renard, M. Verdaguer, L. P. Regnault, W. A. C. Erkelens, J. Rossat-Mignod, and W. G. Stirling, Europhys. Lett. **3**, 945 (1986).
- ⁶ W. Lu, J. Tuchendler, M. von Ortenberg, and J. P. Renard, Phys. Rev. Lett. **67**, 3716 (1991).
- ⁷ J. Darriet and L. P. Regnault, Solid State Commun. **86**, 409 (1993).
- ⁸ T. Yokoo, Y. Sakaguchi, K. Kakurai, and J. Akimitsu, J. Phys. Soc. Jpn. **64**, 3651 (1995).
- ⁹ H. Tsujii, Z. Honda, B. Andraka, K. Katsumata, and Y. Takano, Phys. Rev. B **71**, 014426 (2005).
- ¹⁰ A. Zheludev, Z. Honda, Y. Chen, C. L. Broholm, K. Katsumata, and S. M. Shapiro, Phys. Rev. Lett. **88**, 077206 (2002).
- ¹¹ T. Goto, T. Ishikawa, Y. Shimaoka, and Y. Fujii, Phys. Rev. B **73**, 214406 (2006).
- ¹² S. Sachdev, T. Senthil, and R. Shankar, Phys. Rev. B **50**, 258 (1994).
- ¹³ R. M. Konik and P. Fendley, Phys. Rev. B **66**, 144416 (2002).
- ¹⁴ I. Affleck, Phys. Rev. B **43**, 3215 (1991).
- ¹⁵ E. S. Sørensen and I. Affleck, Phys. Rev. Lett. **71**, 1633 (1993).
- ¹⁶ A. Meyer, A. Gleizes, J.-J. Girerd, M. Verdaguer, and O. Kahn, Inorg. Chem. **21**, 1729 (1982).
- ¹⁷ V. C. Long, Y.-H. Chou, I. A. Cross, A. C. Kozen, J. R. Montague, E. C. Schundler, X. Wei, S. A. McGill, B. Landry, K. R. Maxcy-Pearson, et al., Phys. Rev. B **76**, 024439 (2007).
- ¹⁸ O. Kahn, *Molecular Magnetism* (Wiley-VCH Inc., New York, 1985).
- ¹⁹ S. A. Zvyagin, J. Krzystek, P. H. M. van Loosdrecht, G. Dhaleen, and A. Revcolevschi, Physica B **346-347**, 1 (2004).
- ²⁰ M. Date and K. Kindo, Phys. Rev. Lett. **65**, 1659 (1990).
- ²¹ H. Shiba, T. Sakai, B. Lüthi, W. Palme, and M. Sieling, J. Magn. Magn. Mat. **140-144**, 1590 (1995).
- ²² T. Sakai and H. Shiba, J. Phys. Soc. Jpn. **63**, 867 (1991).
- ²³ M. G. B. Drew, D. M. L. Goodman, M. A. Hitchman, and D. Rogers, Chem. Commun. **20**, 477 (1965).
- ²⁴ M. Sieling, W. Palme, and B. Lüthi, Z. Phys. B **96**, 297 (1995).
- ²⁵ G. Y. Xu, G. Aeppli, M. E. Bisher, C. Broholm, J. F. DiTusa, C. D. Frost, T. Ito, K. Oka, R. L. Paul, H. Takagi, et al., Science **289**, 419 (2000).
- ²⁶ C. Y. Weng, Ph.D. thesis, Carnegie Institute of Technology (1968).
- ²⁷ S. Yamamoto and S. Miyashita, Phys. Rev. B **50**, 6277 (1994).
- ²⁸ T. Manabe, M. Yamashita, T. Ohishi, T. Yosida, Y. Yu, Z. Honda, and K. Katsumata, Synt. Metals **85**, 1717 (1997).
- ²⁹ S. Miyashita and S. Yamamoto, Phys. Rev. B **48**, 913 (1993).
- ³⁰ S. White, Phys. Rev. Lett. **69**, 2863 (1992).
- ³¹ S. H. Glarum, S. Geschwind, K. M. Lee, M. L. Kaplan, and J. Michel, Phys. Rev. Lett. **67**, 1614 (1991).
- ³² M. Hagiwara, K. Katsumata, S. Sasaki, N. Narita, I. Yamada, and T. Yosida, J. Appl. Phys. **79**, 6167 (1996).
- ³³ M. Hagiwara, N. Narita, and I. Yamada, Phys. Rev. B **55**, 5615 (1997).
- ³⁴ J. Z. Lou, S. J. Qin, Z. B. Su, and L. Yu, Phys. Rev. B **58**, 12672 (1998).